Cosmic Rays between the Knee and the Ankle

Maria Giller
University of Lodz, Poland
Email: mgiller@kfd2.phys.uni.lodz.pl

***Abstract*— We summarise the experimental results concerning cosmic rays in the least explored energy region $10^{16} - 10^{18}$ eV. By measuring the extensive air showers produced by these particles effort has been made to determine the primary energy spectrum and the mass composition. We describe the various methods applied to obtain this goal. The main obstacle is the lack of knowledge of the nuclear interactions at super-accelerator energies, which produces a large uncertainty in deducing the mass composition. However, there are methods allowing to determine the energy spectrum practically independently of the interaction model. The increase of the spectrum slope at $\sim 4{\cdot}10^{17}$ eV (by ~ 0.3) looks well established (and can be nicely accounted for if particles were extragalactic), but the quest for the 'iron knee' at $\sim 10^{17}$ eV is worth continuing. The observed flattening of the $< X_{max} >$ just above the ('proton') knee fits well to the scenario of the increasing average mass. Several experiments have been expanding and will hopefully bring more precise data.**

I. Introduction

This paper aims to be a review of the experimental status of cosmic ray research in the primary energy range $\sim 10^{16}{-}10^{18}$ eV. It is the energy region least explored. Below 10^{16} eV there have been extensive studies of the knee structure on the spectrum (at $\sim 4 \cdot 10^{15}$ eV) by many EAS experiments, one of the main results being that the steepening of the all particle spectrum is due to that in the proton (light elements?) flux [1]. The knee region excites a lot of interest, as the change of slope in a (roughly) power law spectrum introduces some characteristic energy scale, helping to pin up hypotheses about CR acceleration and/or propagation. For example, the theory of cosmic ray acceleration by SNRs has been quite well developed and the problem of the highest energy reached by a particle is of great interest and debate.

Above $\sim 10^{18}$ eV there is another obvious feature in the spectrum: at $\sim 4 \cdot 10^{18}$ eV a flattening (the ankle) has been observed by all experiments involved (for a review see e.g.[2]. This highest energy region has been of particular interest since ~ 40 years age when Greisen and independently Zatsepin and Kuzmin predicted a strong decrease in the CR flux above $\sim 5 \cdot 10^{19}$ eV (if of extragalactic origin) due to interactions with the cosmic microwave background. At such high energies one can also expect large CR anisotropies, indicating towards CR sources (Galactic Plane and/or point sources?). So, there have been many papers published on this topic.

However, the region between the knee and the ankle has been of much less interest (in the last ICRC in Pune, in 2005, there were only two groups presenting papers concerning EAS measurements at $\sim 10^{17}$ eV (Tunka [3] and GAMMA [4]; KASCADE-Grande results were preliminary). Probably one of the reasons is not having any well-founded model for CR origin at these energies. One of the few theoretically based motivations to study this energy region is to look for the iron knee at energy ~ 26 times larger than that of the proton knee, that is at $\sim 10^{17}$ eV. Apart from the much smaller CR intensity than at lower energies, the interpretation of the EAS data is much more dependent on the adopted nuclear interaction model - the extrapolation of the accelerator data has to be done by more decades of energy. As the determination of the energy spectrum may not be affected too much, that of the mass composition at these energies does depend on the adopted model quite strongly (see later).

Nevertheless, the situation is not bad: there are experiments studying this energy region and here will to summarize their methods and results.

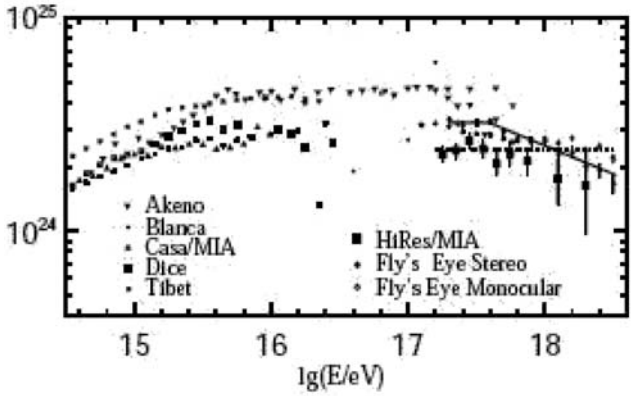

Fig. 1. Energy spectrum of cosmic rays, multiplied by E^3 (in $\mathrm{eV}^2{\cdot}\mathrm{m}^{-2}{\cdot}\mathrm{sr}^{-1}{\cdot}\mathrm{s}^{-1}$, as known in yr 2001. Figure taken from [12]

II. Measuring the energy spectrum

The situation with the determination of the energy spectrum 5 years ago (in 2001) is illustrated in Fig.1. It is seen that the only measurement at $\sim 10^{17}$ eV was that of the Akeno experiment [5], a result published more than 20 years ago! Moreover, the Akeno group measured the CR energy spectrum over 3 orders of magnitude (a record not beaten so far!)

Since then there has been some progress in determining the spectrum and we shall try to compile it and discuss the results.

A. Methods

There are several methods to measure the energy spectrum. One consists in determining the primary energy E_0 for each shower and evaluate the aperture of the array at this energy.

The former is possible only if the measured shower characteristics (or a combination of them) do not fluctuate too much for showers with the same E_0. Such a characteristic is e.g. particle density (or signal in detector) at some distance from the shower core. This method was used first in the Haverah Park experiment [7] and then in Akeno/AGASA [6], where as detectors water tanks and scintillators were used respectively and the signal was measured at 600 m from the core (shower simulations show that particle fluctuations at this distance are smallest for showers around $\sim 10^{17}$ eV). It is worth to note that at these distances it is electrons, photons as well as muons which contribute to the signal, so that a conversion to the primary energy is based on shower simulations, and, as such, on the nuclear interaction model assumed.

Another method is to combine some measured shower parameters in such a way as to get the primary energy. It seems that it is possible to do it, so that the derived primary energy be independent of the primary particle mass. Such a method is used by CASA-MIA [8][9], who combine the number of electrons N_e and that of muons N_μ to get a single parameter $N_e + kN_\mu$ (although measuring these numbers is not a straightforward task). With a suitably chosen value of k (giving a much bigger weight to a small number of muons as compared to that of electrons) this combination is little sensitive to the mass of the primary particle and, what follows, to the interaction model adopted and fluctuations in the shower development in the atmosphere. This is to be expected (as least qualitatively) as the higher the shower develops the smaller N_e and the larger N_μ. Fig.2 illustrates the situation. Although the energy range in question here is below 10^{16} eV (limited by saturation of the scintillator detectors) one can expect that a linear extrapolation of the graph to higher energies would be correct. However, this method has not been used so far for the energies of interest here.

A (somewhat) similar method has been used in the GAMMA EAS experiment [4], situated at 700 g·cm^{-2} (3200 m above sea level). Apart from registering the electromagnetic component of the showers (with 33 large scintillators) this experiment contains a big underground muon 'carpet', consisting of 150 scintillators, measuring muons with $E_\mu > 5$ GeV at the ground. The large height of the observation level (closer to shower maxima - smaller fluctuations and mass/model dependence) allows to estimate E_0 quite well from the shower parameters. Also, from the relatively high energy threshold on E_μ it follows that the number of muons in a shower fluctuates less than that with a lower threshold. As a measure of E_0 the authors use a somewhat complicated expression, depending on the number of charged particles on the ground, number of muons (within $R < 50$ m), shower age and zenith angle. However, by comparing with simulated showers they estimate that the bias at $E_0 > 10^{16}$ eV is smaller than $\sim 5\%$ and the statistical spread is $\sim (10 - 15)\%$.

KASCADE (practically at see level) uses as energy indicator N_μ^{tr} (number of muons between 40 and 200 m from the core), and anyway, they are interested in determining the energy spectra for different mass groups separately (see later). The

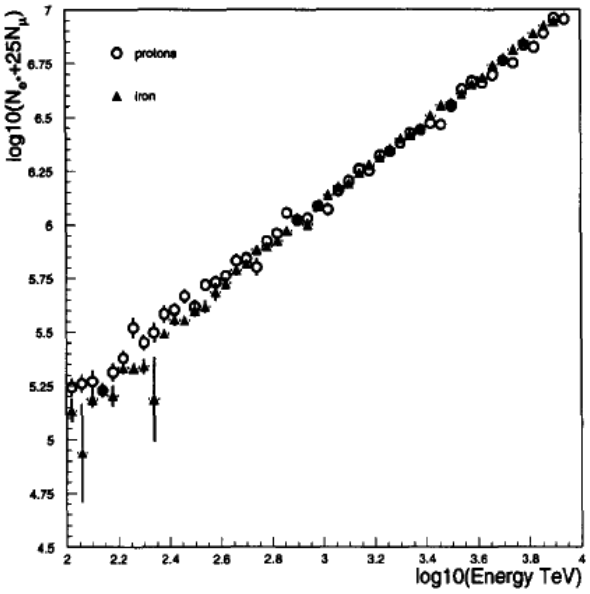

Fig. 2. The energy parameter $N_e + 25 \cdot N_\mu$ as a function of energy for simulated showers from protons and iron. 900 vertical showers for each species. Figure taken from [9]

above methods are limited by the uncertainties of the assumed interaction model and/or those in the determination of N_e and N_μ.

B. Fluorescence light method

It seems that a more accurate determination of E_0 is that by using the fluorescence light technique consisting in measuring the shower image in this light. It can be applied only to energies larger than $\sim 10^{17}$ eV when the fluorescence light signal is large enough to be caught by the mirrors of present sizes (and available costs!) and detected by PMTs of present quantum efficiencies. With this method one can reconstruct the whole (or rather a significant fraction of) the shower cascade curve. Assuming that the fluorescence yield from a charged particle is proportional to the energy deposit of that particle along the same path element (this is what laboratory experiments tell us so far [10], providing also the proportionality constant) one can determine the total energy deposit of the shower in the atmosphere by integrating the deposits over the shower track (seen by consequent PMTs). Thus, the deposited energy can be determined independently of the shower development (providing we measure the light from the most of it), meaning independently of the primary mass, interaction model and shower fluctuations. To obtain the primary energy E_0, however, one has to add to the above the remaining energy of the particles reaching the earth (mainly muons). Simulations show that this term is small (a few %) although model dependent. The main shortcomings of this method are: measurements require dark nights (available at remote sites), transparent atmosphere (and even then its transparency has to be known), absolute calibration of light fluxes. However, the showers can be detected from several

kilometers away, so that the strong decrease of the CR flux with energy is partly compensated by the increase in aperture.

The fluorescence method has been first used by Fly's Eye experiment in Utah (USA) to measure showers at $10^{17} - 10^{18}$ eV [11]. The angular resolution was 5° and the absolute calibration 40%. Since then the group has developed much the precision and sensitivity of their detectors by constructing HiRes (various versions of it). In HiRes-MIA [12] the resolution was 1° and the particle detectors in MIA, measuring the time when a shower hit the earth, allowed a much better reconstruction of the shower geometry (the fluorescence data themselves do not provide a good shower geometry within the shower - detector plane, see e.g. [13]). In HiRes II [14] the field of view has increased (by adding more telescopes) and the accuracy of the timing (by adding FADC which measure signal as a function of time from each PMT). The increased precision of timing caused a better geometrical reconstruction of showers. The authors claim that the absolute calibration is 10% (if true it would be very good indeed!). The problem with the fluorescence method is the difficulty in determining the aperture. Thus the flux uncertainty in this experiment is ∼30%. (Since 2002 HiRes stereo, consisting of two sets of telescopes situated 12 km apart, has been in operation but this is devoted to energy range above that of interest here).

The experimentalists complain that one of the difficulties in the shower reconstructing procedures is the contamination of the fluorescence light by the more abundant Cherenkov light, propagating along the shower but scattered sideways towards the telescopes. However, it has been shown [16][17] that this effect can be allowed for *exactly* if only one knows the age of the shower level from where the light arrives. The shower age at a given depth X (in g·cm^{-2}) in the atmosphere is determined uniquely by the depth of the shower maximum. The Cherenkov light produced at some depth (per unit path) depends only on the energy spectrum of electrons there. It was shown that the shape of this spectrum depends on the shower age only, so that knowing a shower geometry (heights of different levels) and assuming a shower curve $N_e(X)$ one can calculate exactly (once the atmospheric transmission is known) how many fluorescence and Cherenkov photons are emitted towards (and arrive in) the detector. By comparing this with the data one can find the best fitting $N_e(X)$ and/or $dE/dX(X)$.

Fig.3 shows a comparison of the energy spectra obtained by the two fluorescence experiments. The two spectra show the same shapes: consistent with $\sim E^{-3}$ below $\sim 3 \cdot 10^{17}$ eV and steepening to $E^{-3.3}$ above it.

The absolute fluxes agree within the marked uncertainties. The single power law fitted best to the HiRes-MIA data does not describe them well. Thus, we see an evidence of there being a second knee in the energy spectrum! However, it is at an energy factor of ~ 4 higher than that expected for iron nuclei (see above), corresponding to uranium (?!). There is fortunately another explanation, a more plausible one: the steepening could be caused by CR energy losses (on e^+/e^- pair production) during their propagation through the extragalactic sea of the relict microwave photons (see. e.g. [15].)

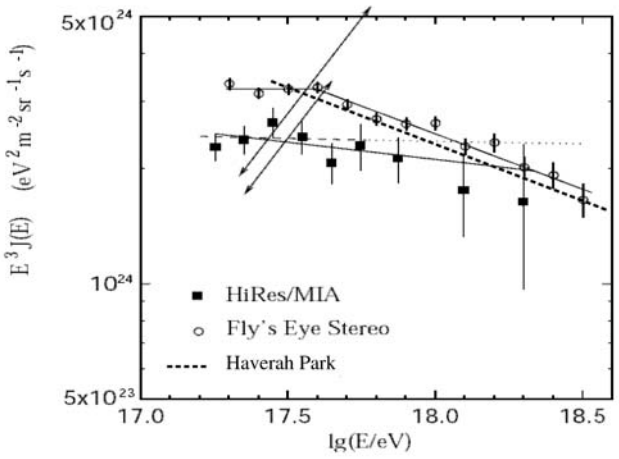

Fig. 3. Comparison of the energy spectra multiplied by E^3 , determined by the fluorescence technique and the new Haverah Park result ([28], see paragraph II D)

C. Air Cherenkov light method

Another method to determine E_0 of a single shower is using the Cherenkov light produced by its electrons (mainly) in the atmosphere. About 36% of electrons [16] are well above the Cherenkov threshold (21 MeV at sea level) producing a pool of light around the shower core. As the number of Cherenkov photons produced by a shower track element is ~ 4 times larger than that due to fluorescence (at sea level) and their flux is collimated along the particle paths, this method can be applied to much lower primary energies (down to $\sim 3 \cdot 10^{14}$ eV). Using Cherenkov light (also with the charged particle data) it is possible to construct some parameters very little sensitive to primary mass and shower fluctuations, depending only on the primary energy E_0. Lindner [21] showed that the slope of the lateral distribution of the Cherenkov density correlates well with the height of the shower maximum, independently of the primary mass. Measuring additionally the total number of charged particles on the observation level, one can scale the slope to E_0. He considered, however, lower energy range and slopes within distances up to ~ 100 m from the shower core. Korosteleva et al. [19] applied this method in the Tunka experiment to larger showers and distances. Fig.4 shows how well N_e/E_0 is correlated with the steepness parameter P of the Cherenkov lateral distribution (ratio of light density at 100 m to that at 200 m from the core). The figure describes showers with various energies and zenith angles. This is, however, a beautiful result of shower simulations (CORSIKA with QGSJet 01). The experimental situation is not that good.

This method has been studied by the QUEST experiment (measuring Cherenkov light) together with EAS-TOP (measuring charged particles) [25] in the same showers and it turned out that the uncertainties in determination of the

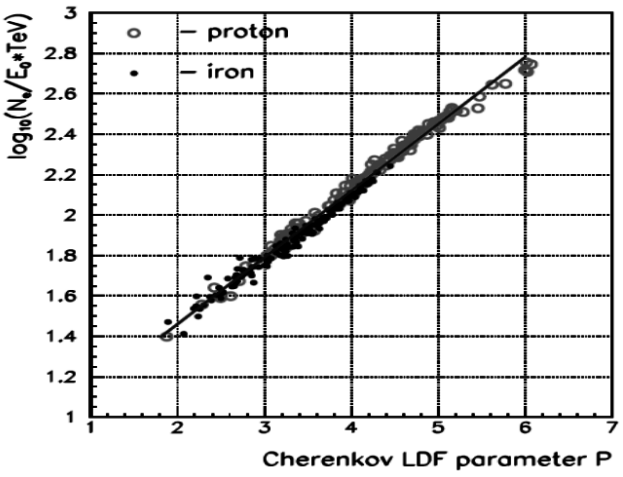

Fig. 4. Correlation between N_e/E_0 and the steepness parameter of the LDF of the Cherenkov light . Simulation results with CORSIKA/QGSJet. Figure taken from [19]

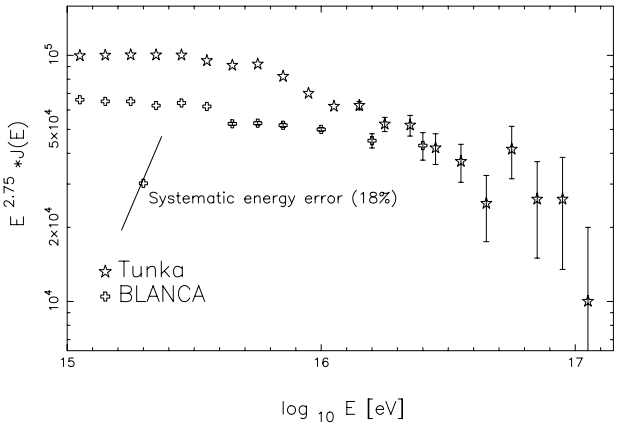

Fig. 5. Comparison of the energy spectra multiplied by $E^{2.75}$ obtained by CASA-BLANCA and Tunka, both by air Cherenkov technique. The difference in slopes is more troubling than the absolute values (see the possible systematic error of CASA-BLANCA)

parameter P are rather large, so that the relative error of the primary energy was $\sim$ 30%. The authors claimed that from the experimental point of view a better method was to use Cherenkov light density at a given distance from the core. This, however, implies performing an absolute calibration of the Cherenkov light detectors, not needed in the previous method. Nevertheless, there were two experiments reaching our energy range of interest: CASA-BLANCA [18] and Tunka EAS Cherenkov experiment [3], using the latter method.

In CASA-BLANCA the charged particle densities (with scintillator detectors - CASA) and those of Cherenkov photons (with large, charge integrating PMT detectors, directed towards the zenith - BLANCA) were measured for each shower (with CASA serving as trigger). The authors MC simulations show that the photon density, C_{120}, at 120 m from the core (for the observation level 870 g·cm^{-2}, corresponding to $\sim$ 1200 m above sea level) is closely related to E_0: $C_{120} \sim E_0^{1.07}$. By fitting "an empirically motivated function" to the lateral distribution of light C_{120} can be determined. The transition to E_0 (assuming a mixed composition) is, however, model dependent, but this uncertainty was estimated as 8% (!?) for the highest energy showers.

A similar method has been used by the Tunka experiment where, however, only Cherenkov light detectors (25 integrating Quasar PMTs and 4 'quick' PMTs to measure pulse shapes) have been installed. The experiment is situated at 675 m – lower in the atmosphere than CASA-BLANCA, so that a measure of the shower primary energy E_0 is the Cherenkov light density at a larger distance from the core (175 m) than that in CASA-BLANCA. Simulations with a mixed composition show [19] a relation: E_0(eV)$= 4 \cdot 10^{14} C_{175}^{0.95}$, where the light density C_{175} is measured in photons cm^{-2}·eV^{-1}. A comparison of the primary energy spectra obtained with the two air Cherenkov experiments is shown in Fig.5. As the difference of the absolute fluxes can be understood (see the error bars marked in the figure), more troubling is the difference of the slopes of the two spectra above the knee. The Tunka group has been expanding their experiment [22] by factor of 10, aiming at 1 km^2 array of Cherenkov light detectors and reaching energies up to $\sim 10^{18}$ eV. Thus, the shower statistics in the $10^{16} - 10^{17}$ eV region will increase significantly and the discrepancy will be hopefully fixed.

D. Particle density/detector signal at a fixed distance from the core

In some experiments it was the signal from a charged particle detector at a particular distance from the shower core that was used as the primary energy indicator. The underlying idea is that while shower development in the atmosphere fluctuates, the lateral distribution of particles gets flatter or steeper, more or less pivoting round some distance. Thus, the particle density at this distance should be closely correlated with the primary energy only. This method was applied for the first time in the Haverah Park experiment, where large water tanks served as the medium for the shower charged particles to emit Cherenkov radiation, to be recorded. The signal depended on the energy carried by the electromagnetic component as well as on the number of muons passing through the water (a combination that can only be predicted by detailed showers simulations). Fig.6 illustrates how the signal at 600 m from the core should depend on E_0 and the primary mass, according to our present knowledge (points), and to that some 20 years ago (line). It is interesting to note that the difference between the present predictions for proton and iron showers ($\sim$ 20%) are smaller than that between the old and the new interaction model ! After the reinterpreting of the Haverah Park data (collected up to some 25 years earlier) with the QGSJet model [23] (now there is still a newest one!) a new energy spectrum was obtained, shown in Fig.3 together with the spectra from the fluorescence detectors. The agreement of the slope above $3 \cdot 10^{17}$ eV is remarkable. Had the lower energy in this experiment been a bit more down, the second

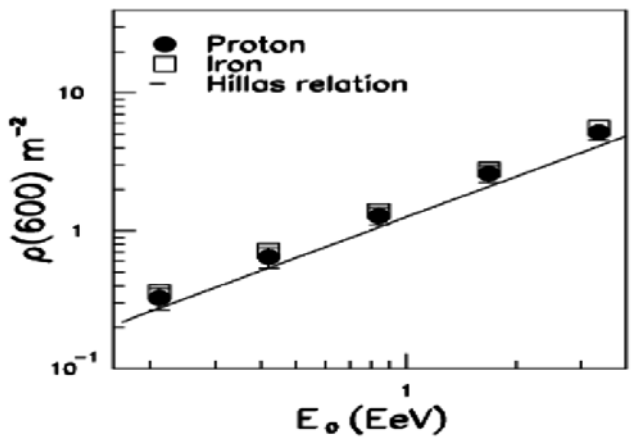

Fig. 6. Detector signal at 600 m from the core (in the Haverah Park experiment) as a function of the primary energy. as simulated with CORSIKA/QGSJet (points) for proton and iron showers at $\theta = 26^{\circ}$. The previous relation used by HP is shown by solid line. Figure taken from [23]

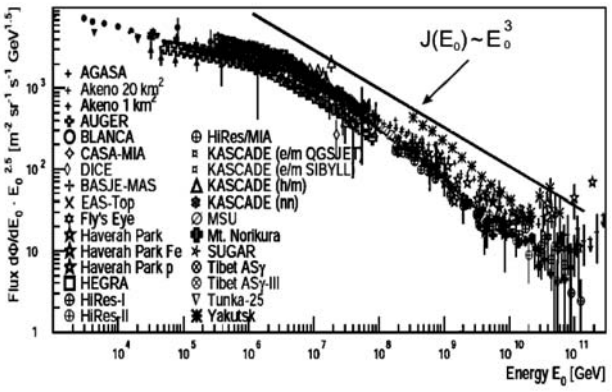

Fig. 7. Compilation of all particle energy spectra, multiplied by $E^{2.5}$ (figure taken from [20]). GAMMA data are compared with KASCADE in Fig.14. The slope -3 is shown by the solid line for comparison. A clear difference of the slope below and above $\sim 4 \cdot 10^{17}$ eV is seen

knee would have probably been observed many years earlier.

It was, however, the Akeno experiment [5][6] that covered many orders of magnitude in the energy spectrum (as mentioned above) and indicated in 1992 that the spectrum steepens again at $\sim 4 \cdot 10^{17}$ eV. Measuring the energy spectrum in a large energy range by a single experiment requires special geometrical design and trigger. The Akeno experiment (up to 20 km^2) was actually a combination of several arrays with different geometrical scales and corresponding triggers and, together with AGASA (100 km^2), was able to cover cosmic ray energies from $\sim 3 \cdot 10^{14}$ eV up to their highest end.

We only want to concentrate here on the inner energy region. With the Array 20 (20 km^2) the method of determination of E_0 was based on measuring S_{600}, particle density (as measured by the scintillator detectors) at 600 m from the shower core. A conversion to E_0 was based on (the best at that time) Monte Carlo simulations, weakly depending on the primary mass [24]. The energy spectrum was also determined independently with Array 1 (1 km^2) by measuring the total number of electrons in the shower N_e (see below), and the primary energies differ by 15%. Both spectra show an increase of slope from about $\gamma = -3.0$ above the first knee to -3.3 above $\sim 4 \cdot 10^{17}$ eV.

E. Other methods

As an example of another method we want to recall the just mentioned one, applied by the Akeno group based on N_e. Although it is rather old but we want to add it here for some completeness. As it is well known the total number of electrons at the shower maximum N_{max} is a very good indicator of E_0, being almost independent of the primary mass or interaction model. To derive it from the measured N_e the measurements of shower longitudinal development on Mount Chacaltaya (at the depth of about half thickness of the atmosphere), obtained with constant intensity cut method, were used. Recalculation of N_{max} to E_0 based on simulations gives ~ 1.4 GeV per particle, slightly increasing for smaller showers.

Still another approach is aiming at a determination of the energy spectra for different elemental groups, rather than that of all the particles. This is the method used by the GAMMA and KASCADE experiment groups. However, as it refers to the primary composition, we postpone this topic to paragraph III.

F. All particle energy spectrum

Fig.7 shows results obtained by the described above experiments, together with some others. The straight line above the experimental points shows the slope -3. By comparing the data with it it is clear that while the slope just above the knee at $\sim 4 \cdot 10^{15}$ eV coincides with -3, above $\sim 4 \cdot 10^{17}$ eV it is steeper. As to the absolute fluxes multiplied by $E_0^{2.5}$ they differ by not more than a factor of $2 - 2.5$ (not counting the Yakutsk data). With the actual slope of the energy spectrum it corresponds to the absolute energy discrepancies (assuming no error in the flux itself) of $\sim 30\%$, a result not bad keeping in mind that flux measurements do add to this number.

Unfortunately (?) there does not seem to be any feature at 10^{17} eV, so that the expected iron knee probably will not show up. However, more precise measurements coming up (e.g. KASCADE-Grande, Chacaltaya, Tunka) might discover some features smeared so far.

The change of slope at $\sim 4 \cdot 10^{17}$ eV is clearly visible. An interesting interpretation of it (proposed e.g. by Berezinski et al [15]) is that the cosmic rays in this region are of an extragalactic origin. As such they suffer energy losses on the universal microwave radiation and at that energy it is the electron/positron pair production which starts coming into play, steepening the power law source spectrum. (This scenario implies of course that there should be a dramatic decrease of the extragalactic flux above $\sim 4 \cdot 10^{19}$ eV, the GZK cutoff, due to pion production on the same microwave background). As we do not want to go too much into the origin details here, we only notice one weak (?) point of this model: it requires a rather flat source spectrum reaching the observed flux level just

below 10^{18} eV, so that the Galactic component (dominating at lower energies) has to cut-off at roughly the same energy.

III. Mass composition

A. Methods

To determine the mass of the primary particle for a single shower is rather impossible (at least to distinguish between various nuclei). It would have been so even if we had known well the interaction model, because of large fluctuations in the development of its nuclear cascade. It is, however, not so hopeless in trying to determine some average mass, or, as it is largely done, average $\ln A$, where A is the mass number of the primary nucleus ($\ln A$ is closely related to the depth of shower maximum X_{max}, a measurable quantity). Here we shall discuss the methods used in the mass composition determination.

Most methods are based on the shower property that if initiated by a heavy nucleus it will develop in the atmosphere higher (on average) than that initiated by a light one with the same primary energy. A nucleus with energy E_0 consist of A nucleons, each with energy E_0/A. As the depth of the shower maximum X_{max} is proportional (roughly) to the logarithm of the nucleon energy (at least it is so in the superposition model), the larger A the higher the shower develops (the smaller X_{max}). Thus, one method is to determine X_{max}. To do so direct observations of the shower curve with the fluorescence method seem the best, notwithstanding all the inconveniences (see above).

The larger is the mass of the primary particle the more muons there will be at the ground for two reasons: a) the average energies of pions are smaller, so that more of them decay rather than interact, and b) the shower develops in a thinner atmosphere so that the number of decaying pions increases even more. Thus, measuring the muon number N_μ in a shower (for showers with known E_0, the problem to be solved, but see above) is another method to tell about the primary masses. Often a better way (from the experimental point of view) is to determine number of muons within a restricted distance from the shower core (as KASCADE did, determining N_μ^{tr}).

There are also other methods based on a higher development of more 'massive' showers: the shape of the lateral distribution of Cherenkov light has been found to be closely correlated with the height of shower maximum above the observation level [21], so that measuring the slope of this distribution leads to a determination of X_{max}. Applying the Cherenkov light method leads, however, to the same inconveniences as with the fluorescence light (see above).

Yet another way is to apply the so called "constant intensity cuts": finding the dependence of N_e on zenith angle for showers having the same intensity one actually studies the behaviour of $N_e(X)$ for showers with the same E_0. However, to observe showers at their maxima (or even better – above them) it is necessary to go to high mountain altitudes (as does the Chacaltaya group, see later). There is one method, however, that is not based on the dependence of average X_{max} on A, but on the fluctuations of X_{max} in single showers.

A shower initiated by a nucleus with mass number A (fragmenting into nucleons after several collisions) behaves (more or less) as A showers developing independently. In the superposition model such a shower is just a sum of A showers, each with primary energy E_0/A. It is easy to show that, if the single shower curve $N_e(X)$ can be well approximated around its maximum by a parabola (as each differentiable curve can be), then X_{max} for the sum of the showers coincides with the average of X_i (the depths of the maximum for the A subshowers). Thus, the dispersion of $X_{max}(E_0,\, A)$ should be smaller by factor $A^{1/2}$ than that of $X_{max}(E_0/A,\, 1)$. We can compare it with the results of simulations (Fig.8 [26]). According to the superposition model the ratio of the latter to the former should be $56^{1/2} = 7.5$, whereas at $E_0 = 5.6 \cdot 10^{17}$ eV it equals ~ 3.5. So, the superposition model does not describe well fluctuations of X_{max} in iron showers in neither of the interaction models. They are twice as big than predicted. However, they are smaller than in proton showers and, as such, can serve as an indication of the primary masses, whether they are light or heavy. The situation would get worse if there was a mixture of those, say protons and iron nuclei. In principle this could occur when a Galactic iron component (dying with energy) adds to the extragalactic protons. Then the X_{max} fluctuations would be even larger than those for pure proton flux. But (depending on their relative fractions) it could be perhaps possible to distinguish the two components if detailed measurements of the shape of the X_{max} distribution were possible.

A good information about the primary masses could be gained by registering high energy hadrons in a shower. In a proton initiated shower the highest energies of hadrons should be much larger than those in an iron shower. Detecting hadrons is however more difficult than electrons and/or muons: having larger energies the hadrons are more concentrated around the shower core, so that their detection area is much smaller. Moreover, to tell about the primary mass, one would have to measure also their energies, what implies building large, costly calorimeters.

We would also like to mention a method developed in the Auger experiment, where water tanks are used as particles detectors on the ground. A mixture of electrons, gamma quanta and muons add to produce Cherenkov light signal.

By studying the time shapes of this signals it is possible to draw conclusions about the fraction of muon component: muons, being more energetic than electrons and gammas, have trajectories less scattered, so arrive to the ground earlier. The larger their fraction the shorter the rise time of the signal. Here, however, measurements with Flash ADC are necessary, probing the signal every short time bin (25 ns in Auger).

To summarise, let us stress that, while there are methods to determine the primary energy E_0 in a model independent way (see above), the conclusions about primary masses are always based on a particular model of strong interactions at high energies. However, from the dependence of X_{max}

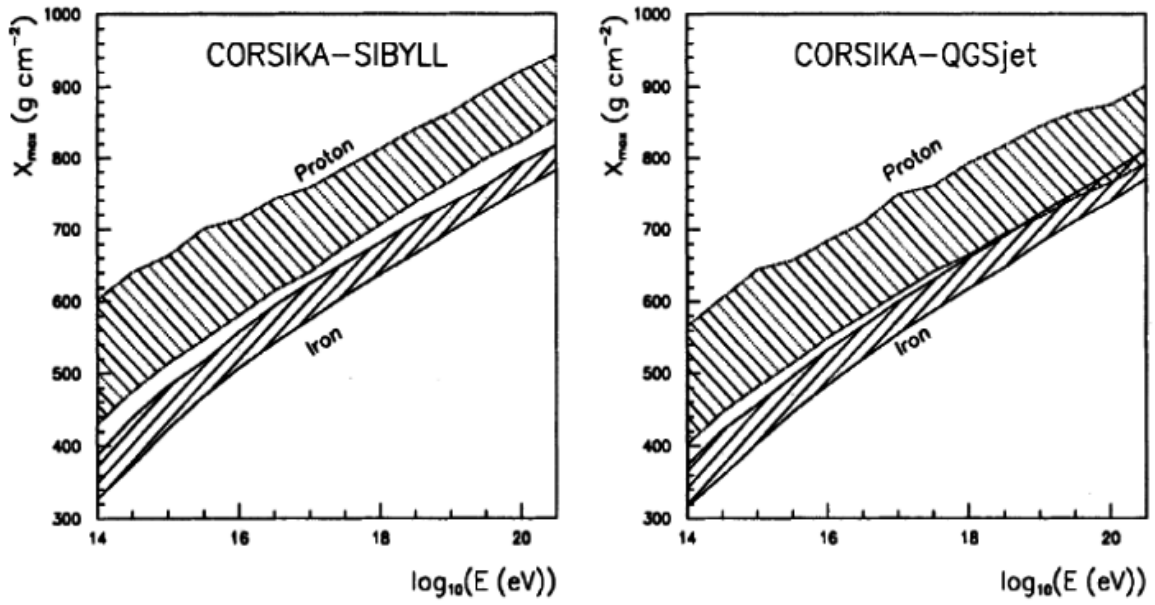

Fig. 8. X_{max} as a function of energy, results of simulations. The hatched areas show 68% of the distribution . Figure taken from [26]

on $\log(E_0)$ (the elongation rate) it seems to be possible to determine whether the mass composition changes with E_0 in a way little depending on the model (see below).

B. Measuring X_{max} and its distribution

As it was already mentioned, applying the fluorescence method to study these parameters is possible for showers above $\sim 10^{17}$ eV. There were two experiments: Fly's Eye [11] and HiRes-MIA [12], described shortly above, which measured X_{max} of showers below 10^{18} eV (there are HiRes I and HiRes II, but they have been measuring showers above 10^{18} eV). In Fig.9 the X_{max} distributions, obtained by HiRes-MIA experiment are presented for three energy bins. There are also shown the corresponding distributions calculated for primary proton and iron, with QGSJet 01 model. It is obvious that none of them reproduces the data (however, it would be interesting to see how a single intermediate nucleus, like carbon or oxygen, compares to the data). Assuming a two component composition (protons and irons only) the authors obtain an increase of the proton fraction with energy (from ~ 0.5 to ~ 0.9). A similar result could be obtained from studies of the average X_{max}. The dependence of $< X_{max} >$ on energy, obtained by the two experiments, together with those operating at lower energies, is shown in Fig.10 (taken from [12]). A constant elongation rate has been subtracted from $< X_{max} >$ and this is on the vertical axis. Here again, HiRes-MIA claim to observe a transition from heavier to lighter composition above $\sim 10^{17}$ eV.

The Fly's Eye data, however, seem to show an increase of a light component only above $\sim 10^{18}$ eV (and a slight decrease of it for $10^{17} \div 3 \cdot 10^{17}$ eV !?). In a more recent paper [27] the HiRes group concluded that a shift of the Fly's Eye $< X_{max} >$ values by 13 g·cm^{-2} (compensating for an apparent systematic error) puts all the fluorescence data in a reasonable agreement. However, there will still remain differences in $< X_{max} >$ between the two experiments reaching as much as ~ 40 g·cm^{-2}.

C. Lateral distribution of air Cherenkov light

This method also uses information about X_{max} to conclude about primary masses but it is not measured directly but determined by the shape of the lateral distribution of Cherenkov light emitted by showers. As discussed above there were two experiments, CASA-BLANCA and Tunka, which measured the lateral distribution of the air Cherenkov light.

CASA-BLANCA fits this distribution for each shower by an exponential function $\sim \exp(-s \cdot r)$ in the distance region 30–120 m. According to their shower simulations, the slope s of this distribution is practically linearly related to X_{max}. It is a pity that the authors did not show the relevant simulation results. One can, however, get an idea about the strength of this correlation from simulations done by Lindner [21] at lower energies. Fig.11 presents scatter plots in the plane: distance from the observation level to the shower maximum vs slope s. There are separate figures for two primary energies ($3 \cdot 10^{14}$ and $5 \cdot 10^{15}$ eV) but the best fitting line depends on E_0 very little (see the right figure). Neither does it depend on the primary mass, so it is as well model independent. The resulting $< X_{max} >$ as a function of E_0 (see above how E_0 was determined) is shown in Fig.12. There is a clear flattening of the CASA-BLANCA points at about $5 \cdot 10^{15}$ eV, the energy coinciding with the knee in the energy spectrum. According

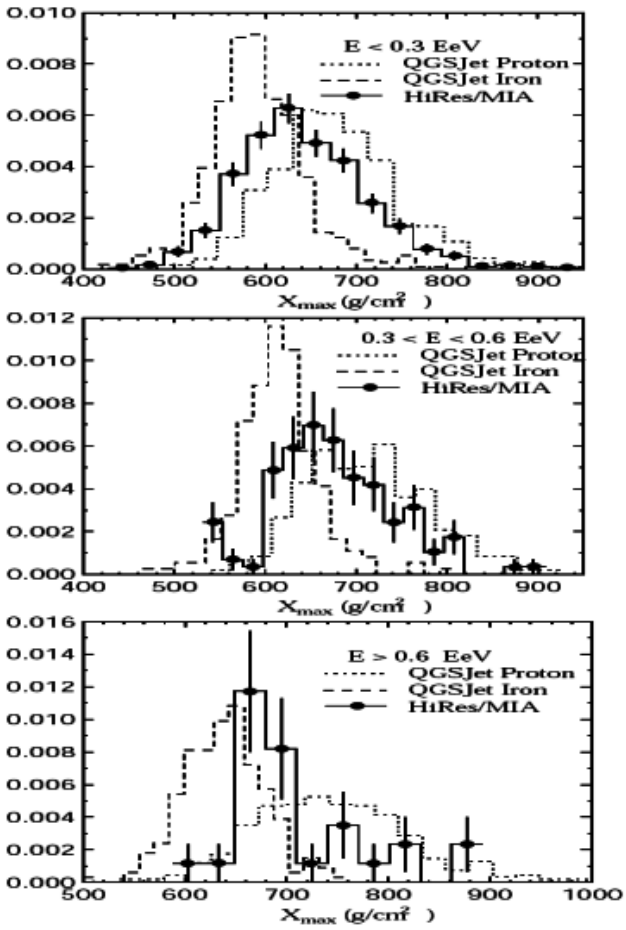

Fig. 9. X_{max} distributions for three energy bins, as obtained by HiRes-MIA (points with error bars). Predictions for pure proton and pure iron composition are also shown

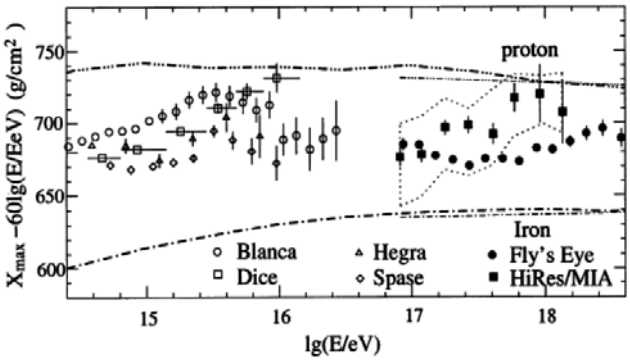

Fig. 10. $< X_{max} >$ – 60 g·cm^{-2} · log(E/1 EeV) as a function of energy (from [12]). Reanalysis of the Fly's Eye data [27] shifts their points by 13 g·cm^{-2} up

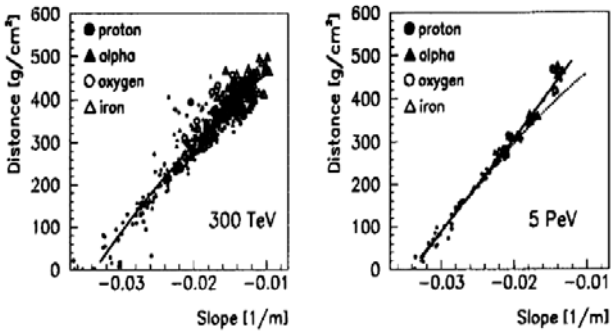

Fig. 11. Scatter plot for distance to the shower maximum from the observation level (in g·cm^{-2}) and slope s of the lateral distribution of Cherenkov light (from [21]). Simulations for two primary energies. A very good correlation of the two parameters, independent of the primary mass is seen, particularly for the higher energy

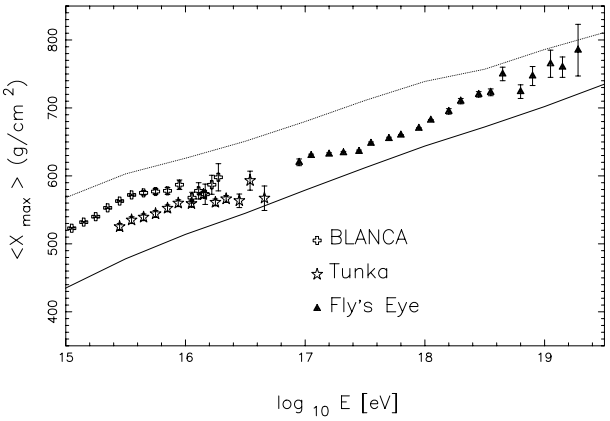

Fig. 12. $< X_{max} >$ as function of primary energy, as determined by the three experiments by air Cherenkov (Tunka and CASA-BLANCA) and fluorescence technique (Fly's Eye)

to KASCADE data and analysis [1] this knee is caused by a kink in the proton spectrum, so that the average mass should increase above it. It seems to have been confirmed by CASA-BLANCA (however, the lightening of the average mass in the region $\sim 3 \cdot 10^{14} - 3 \cdot 10^{15}$ eV seems to be at odds with the KASCADE data). Although the transition from $< X_{max} >$ to the mean mass is model dependent this conclusion holds for any model, providing no drastic changes in the interaction characteristics are introduced.

The authors of the Tunka experiment [3] also find a good correlation between the position of X_{max} and the slope of the Cherenkov lateral distribution. However, they represent the distance to the shower maximum, H_{max}, in kilometers rather than in g·cm^{-2} and the slope as the ratio of the Cherenkov density at 100 m to that at 200 m. They find that H_{max} can be well represented by a quadratic function of the slope, practically independent of anything (E_0, mass, zenith angle). (It would be worth checking which one of the two correlations, this one or that used by CASA-BLANCA, it a better one. Of course, changing g·cm^{-2} into km will not change the correlation coefficient, but the slopes are defined differently

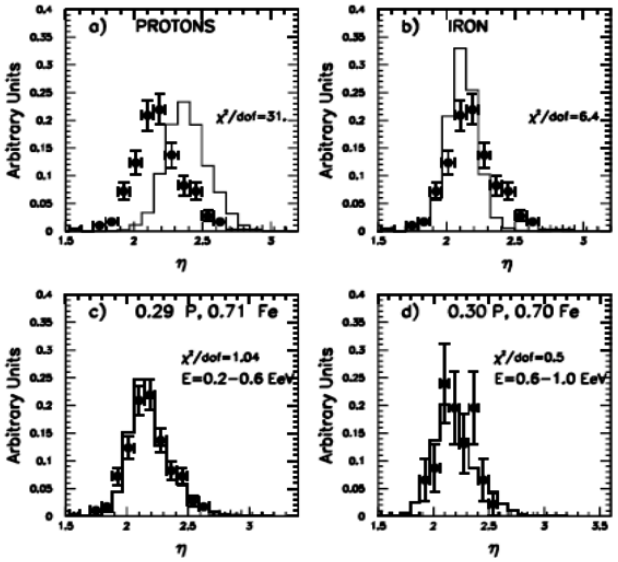

Fig. 13. Distributions of the slope η (see text) of the lateral distribution of the signal in the Haverah Park experiment (points). Also shown predictions for different primary masses

and correspond to different regions of the core distances and one of them could be better correlated with the shower maximum position.)

It is interesting to see the comparison of these results with those of CASA-BLANCA. The general behaviour of $< X_{max} >$ with $\log(E_0)$ is the same: it increases more or less linearly, flattens (almost completely!) in an energy region of factor ~ 3, to increase again. The value at which $< X_{max} >$ flattens is the same in both experiments, but the energy is not. A shift by a constant factor in energy would put in a very good agreement both $< X_{max} >$ curves, but it would not help to do it with their energy spectra which have different slopes (see above and Fig.5).

D. Lateral distribution of shower particles

Haverah Park, working at higher energies, used the shape of the lateral distribution of the signal in the detector as a measure of the mass composition [23]. The detectors were water tanks with PMTs measuring the Cherenkov light produced in the water by a mixture of electromagnetic and muon components. The steepness η of the signal lateral distribution (fitted by $\rho(R) \sim R^{-(\eta - R/4km)}$) was measured accurately for each selected shower by the denser part (infill array) of the whole array. The obtained distributions of η for showers with primary energy in two energy bins: $(2-6)\cdot 10^{17}$ eV and $(6-10)\cdot 10^{17}$ eV (E_0 determined from $\rho(600)$, see above) are presented in Fig.13. Also shown are predictions for proton and iron showers, based on QGSJet 98 model. In the first energy bin a perfect fit is obtained for a simple mixture of 29% protons and 71% irons. The error bars in the second bin are rather large, but the best fit corresponds to the same composition.

However, these numbers turn out to be quite sensitive to the interaction model. The predictions with the QGSJet 01 model increase the proton fraction to 48% (by 40%). One has to keep in mind that these fractions depend much on the number of mass components used and their masses. It seems that η distribution for the first energy bin could be accounted for by some iron and (say) carbon mixture. The authors checked also the applicability of the signal shape (more precisely - the signal rise time) to the mass composition determination. However, in this energy range (unlike at $> 10^{19}$ eV, as in Auger) the method seems to be not sensitive enough.

IV. Determination of the energy spectra for different mass groups

There have been two experiments which state the problem slightly differently than these described above: their aim is to determine the energy spectra for several, defined in advance, mass groups simultaneously. These are the GAMMA experiment [29] and KASCADE [1]. The main idea is to fit the relative abundances of several mass groups as to reproduce best the multidimensional distributions of the observed shower parameters. Some form of the searched for energy spectra may or may not be assumed (see later). As the final results of the two experiments do not agree it is worth to analyse the similarities and differences between them hoping to find the reasons for the disagreement.

As already described, GAMMA is a mountain experiment, situated (in Armenia) at a depth of 700 g·cm^{-2}, whereas KASCADE is almost at see level (1022 g·cm^{-2}). Both experiments measure the electromagnetic component of showers with scintillators, KASCADE in the range $10^5 < N_e < 10^7$, GAMMA - in that almost one order of magnitude larger; thus, their primary energy range is practically the same: $10^{15} - 10^{17}$ eV. Both measure also muons, but in a quite different way. In GAMMA there is 'the muon carpet', a compact area of 150 m^2, covered with scintillators, located underground just below the center of the surface detectors and corresponding to $E_\mu > 5$ GeV. Muon detectors in KASCADE (those used for the composition analysis) are spread on a larger surface, with spacing of 13 m, and the energy threshold, 230 MeV, is much lower. At the depth of GAMMA these muons would have energies about 1 GeV. So, the two experiments chose, for their composition analyses, muons in the energy ranges different by factor ~ 5.

KASCADE fits shower simulation results, assuming 5 primary mass groups (p, He, C, Si and Fe) to the two-dimensional, experimental distribution (N_e, N_μ^{tr}), where N_μ^{tr} is the number of muons between 40 m and 200 m from the shower core. GAMMA choses 4 masses (p, He, O and Fe) and fits several many dimensional distributions - up to the one in the four- dimensional space (N_{ch}, N_μ, s, $\cos\theta$), where s is the free parameter in the Nishimura-Kamata lateral distribution function of electrons and θ is the shower zenith angle. KASCADE does not assume any form of the energy spectra in advance, whereas GAMMA does assume that the elemental spectra in rigidity are all the same.

A comparison of the results of the two experiments is shown in Fig.14 and 15, taken from their original papers. Although the all particle spectra agree quite well (see also [29]), there are

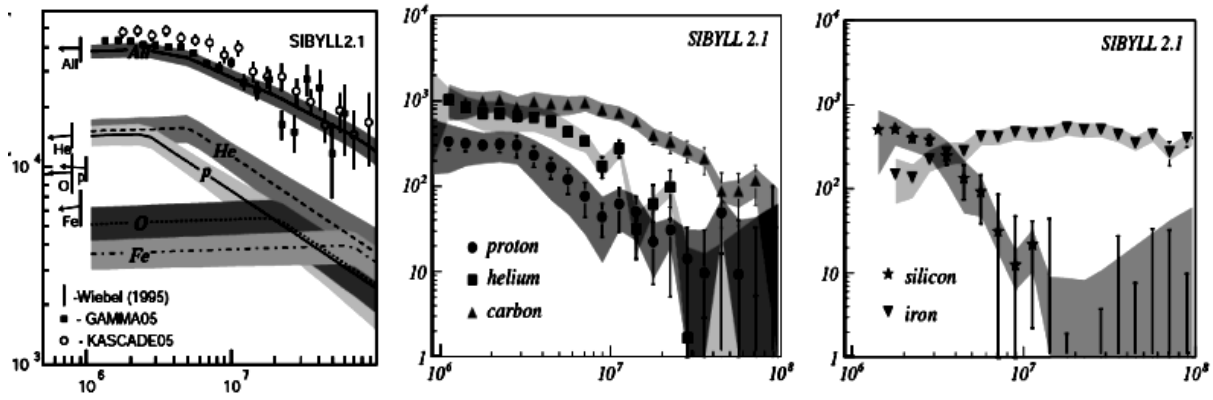

Fig. 14. Energy spectra (in $m^{-2}\cdot s^{-1}\cdot sr^{-1}$) for elemental groups. Left spectra obtained by GAMMA [4] are multiplied by $E(\mathrm{GeV})^{2.7}$. Middle and right spectra from KASCADE [1] multiplied by $E(\mathrm{GeV})^{2.5}$. Sibyll model

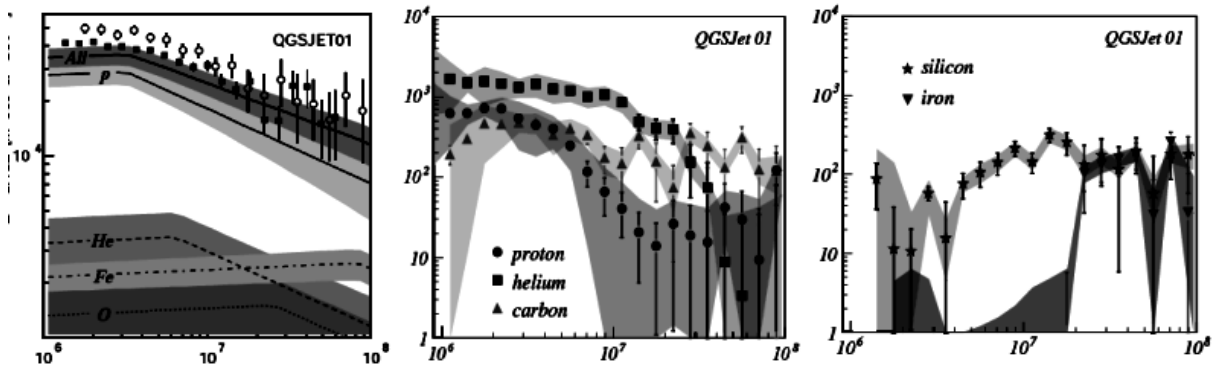

Fig. 15. The same as in Fig.14 but for QGSJet 01 model

large discrepancies between the single mass spectra deduced by both groups. For the QGSJet 01 model GAMMA obtains mainly protons, with the rest of nuclei being each about one order of magnitude less abundant. However, KASCADE gets comparable fluxes of protons, helium and carbon group, with a quite considerable contribution of silicon group at 10^{16} eV. The Sibyll 2.1 model gives different results (what may be understandable) but again, the deduced compositions from the two experiments are different. A bit striking is the dominance of carbon nuclei below 10^{16} eV obtained by KASCADE. However, for each model KASCADE gets a steepening in the proton and helium spectra, without assuming it. For the Sibyll model the positions of the steepening correspond quite well to the same rigidity for p, He and C but not for Si.

In general, GAMMA gets a lighter composition than KASCADE does. Could it be because they base their conclusions on muons with different (higher) energies? KASCADE did a check of the interaction models based on muons with different energy thresholds and on the measured hadron component [30] concluding that no interaction model is able to describe their all data. Their highest muon energy threshold is 2.6 GeV, which at the GAMMA level of 700 $g\cdot cm^{-2}$ would be ~ 3.3 GeV (in near-vertical showers considered by both groups). This is almost the GAMMA muon threshold (5 GeV) and it would be interesting if KASCADE derived the composition basing on those highest energy muons. It would probably be not the same as that based on the lowest energies, as the various component data from KASCADE alone can not be described consistently by any of the two interaction models with any composition. So, perhaps one should not be surprised too much that the conclusions about composition from the two experiments do not agree.

The reason for the disagreement lies most probably in the inadequacy of the interaction models used. QGSJet 01 model assumes the quickest growth (with energy) of the multiplicity of particle production. The total number of muons produced is then larger that that in the Sibyll model. However, the > 230 MeV muons, to be compared with KASCADE data at sea level, would be produced low in the atmosphere (up to ~ 3 km because of decay) where the hadronic cascade would be already weak. Thus, their increase (if at all) will be smaller than that of muons with higher energies, observed by GAMMA. Then, basing on QGSJet 01, GAMMA predicts lighter composition than KASCADE does. This possible explanation is compatible with the fact that the predictions of the two experiments are less divergent for the Sibyll 2.1 model. As now showers develop deeper in the atmosphere, the above effect is weaker and this situation seems to be closer to reality. It follows from the above how important it is to measure as many shower characteristics as possible, so as to have cross-

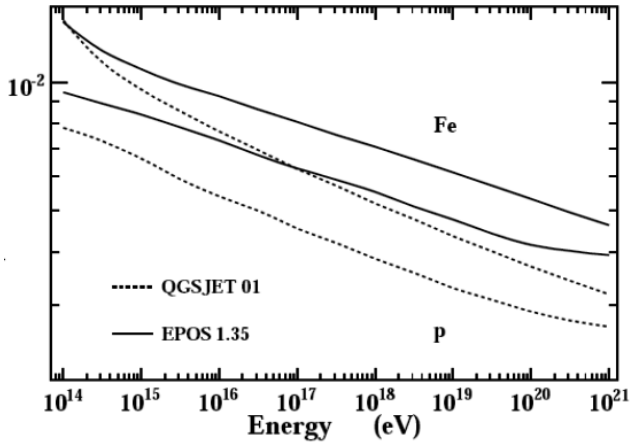

Fig. 16. Ratio of the total number of muons in a shower at ground to the primary energy (in GeV) as a function of primary energy for proton and iron primaries. QGSJet 01 and EPOS models [33]. It is seen that at 10^{17} eV number of muons in a proton shower for EPOS equals to that in an iron shower in QGSJet 01!

checks of the model/composition conclusions.

V. A COMMENT ON INTERACTION MODELS

We have seen that the interpretation of the shower data in terms of the mass composition is strongly dependent on the interaction model used. It seems that unless there is a realistic model, describing correctly the depth distribution of the production of muons with different energies in a shower, with respect to that for electrons (not mentioning hadrons), the conclusions about the mass composition will not be reliable. However, as the prospects of measuring the high energy interaction characteristics are not that close (despite the approaching advent of LHC) one is striving to deduce the primary masses without knowing the exact interaction model.

A way of disentangling the two unknowns may be based on the phenomenon of the leading hadron, believed to occur also at the extra-accelerator energies. Thus, measuring energy spectra of hadrons (both in showers as those uncorrelated with them), at best at mountain altitudes, would bring useful information about the composition.

Our present knowledge about the high energy interactions does not allow us to draw satisfactory conclusions even about the average $\ln(A)$. New improvements have recently been applied to QGSJet 01, resulting in QGSJet II [31][32]. The latter predicts $\sim 20-30\%$ less muons for proton showers with $10^{16}-10^{18}$ eV and $< X_{max} >$ larger by about $20-30$ g·cm^{-2}. On the other hand a new model, EPOS, appeared lately [33] allowing for a more abundant (anti)barion pair production and thus increasing number of muons produced in a shower. Just to illustrate how different may be the predictions of the models used for composition conclusions, we show a comparison of N_μ/E_0 predicted for proton and iron showers (Fig.16, taken from [33]). EPOS model predicts the same number of muons for proton showers as QGSJet 01 for iron in our energy range! A comparison of EPOS results with the new QGSJet II would be even worse. We will most probably profit from the LHC results, corresponding to $\sim 10^{17}$ eV p-p laboratory energy, to improve our models.

VI. CONCLUSIONS AND FUTURE PROSPECTS

We have chosen the primary energy region to discuss here in a somewhat artificial way, the main reason being, however, to fil a gap in the interest of cosmic ray community.

There are methods enabling to determine the primary energy spectrum of all particles in a way little dependent on primary masses. Although the number of experiments is relatively small the determination of the change of slope at $\sim 4 \cdot 10^{17}$ eV seems to be quite convincing ($\gamma = 3.0 \pm 0.1$ below this energy and $\gamma = 3.3 \pm 0.1$ above it). This occurs, however, at the energy a factor of ~ 4 higher than that expected for 'the iron knee', equal to $26 \cdot 4 \cdot 10^{15}$ eV $\cong 10^{17}$ eV.

We can expect new measurement results rather soon. Chacaltaya has been expanding the array by factor of ~ 10 to be able to detect enough statistics of showers $> 10^{17}$ eV [34]. As it is situated at 550 g·cm^2 it will be able to observe showers at their maximum, where the electromagnetic size is a very good indicator of the primary energy (small fluctuations). Other mountain experiments which have been expanding are Tunka [35], and Tibet [36]. So, the existence of the second knee at $\sim 4 \cdot 10^{17}$ eV will surely be checked soon.

There are methods to determine X_{max} of single showers, the distribution of which is very useful in finding mass composition. However, the transition from $< X_{max} >$ to $< \ln A >$ depends rather strongly on the interaction model used. As there are several different models, extrapolated by many orders of magnitude from the accelerator data, there is no agreement concerning $< \ln A >$ in our energy range.

However, the $< X_{max} >$ dependence on E_0 (elongation rate) has an interesting feature, being practically flat through about one order of magnitude, starting just at the knee energy. This would nicely fit the picture of there being an increase of the mean mass in this energy region, compensating the deepening of the shower development with energy. This behaviour of the elongation rate needs further confirming, as it is of important consequences.

KASCADE does not determine the composition by X_{max} but by fitting the (in advance adopted) mass groups to the frequency histogram on the (N_e, N_μ^{tr}) plane, using only the lowest energy muons. This method is, of course, model dependent as well. All their valuable data, concerning muons above two other, higher energy thresholds and those on hadrons, seem to indicate that none of the model used is able to describe them well with any composition. It is quite probable that this is a reason of the different composition obtained by GAMMA. However, one should try to (and probably could) solve this puzzle in the near future, with new data coming soon from LHC and new cosmic ray experiments.

KASCADE-Grande, with the area ~ 10 times larger than that of KASCADE, has already been taking data and producing preliminary results [37]. As their main goal is to look for

the iron knee, they will surely analyse the data carefully to produce valuable results on the energy spectrum.

Needless to say that all the effort described above is made to solve the problem of the cosmic ray origin. To reach this goal there is also a need for theoretical work. Decently speaking, there is no plausible theory (or model) of the cosmic ray origin in this energy region. Various energetic phenomena are suspected to be responsible for charged particle acceleration to cosmic energies: SNRs, pulsars, microquasars, shocks in extragalactic jets and so on. Of course, when searching for cosmic ray origin it would be unwise to limit oneself to a particular (two orders of magnitude) range of energy, as here. This problem has to be approached keeping in mind all the cosmic ray energy range.

ACKNOWLEDGMENT

The author thanks the organisers of the 20th European Cosmic Ray Symposium in Lisbon for inviting her to give a talk on this subject (this is an extended version of this talk).

This work was also supported by the grant no 1 P03 D01430 of the Polish Ministry of Science and Higher Education.

REFERENCES

[1] T. Antoni et al., Astropart. Phys. 24 (2005) 1.
[2] M. Nagano and A.A. Watson, Rev. Mod. Phys. 72 (2000) 689.
[3] N. M. Budnev et al., in Proc. 29th Int. Cosmic Ray Conf., Pune, 6 (2005) 257.
[4] S.V. Ter-Antonyan et al., in Proc. 29th Int. Cosmic Ray Conf., Pune, 6 (2005) 101 and 105.
[5] M. Nagano et al., J. Phys. G, 10 (1984) 1295.
[6] M. Nagano et al., J. Phys. G,18 (1992) 423.
[7] M. A. Lawrence, J. O. Reid and A. A. Watson, J. Phys. G, 17 (1991) 733.
[8] M. A. K. Glasmacher et al., Astropart. Phys. 10 (1999) 291.
[9] M. A. K. Glasmacher et al., Astropart. Phys. 12 (1999) 1.
[10] F. Kakimoto, E. C. Loh, M. Nagano, H. Okuno, M. Teshima and S. Ueno, Nucl. Instr. Methods Phys. Res. A 372 (1996) 527.
[11] D. J. Bird et al., Ap. J. 424 (1994) 491.
[12] T. Abbu-Zayyad et al., Astrophys. J. 557 (2001) 686.
[13] P. Sommers, Astropart. Phys. 3 (1995) 349.
[14] R. U. Abbasi et al., Astropart. Phys. 23 (2005) 157.
[15] V. Berezinski, A. Gazizov and S. Grigoreva, Phys.Rev. D 74 (2006) 043005.
[16] M. Giller, G. Wieczorek, A. Kacperczyk, H. Stojek and W. Tkaczyk, J. Phys. G, 30 (2004) 97.
[17] M. Giller, A. Kacperczyk, J. Malinowski, W. Tkaczyk and G. Wieczorek, J. Phys. G, 31 (2005) 947.
[18] J. W. Fowler et al., Astropart. Phys. 15 (2001) 49.
[19] E. E. Korosteleva, L. A. Kuzmichev, V. V. Prosin, B. K. Lubsandorzhiev and the EAS-TOP Collaboration, Int. J. Mod. Phys. A, 20 (2005) 6837.
[20] J Hörandel, astro-ph/0508014.
[21] A. Lindner, Astropart. Phys. 8 (1998) 235.
[22] D. V. Chernov et al., Int. J. Mod. Phys. A, 20 (2005) 6796.
[23] M. Ave, J. Knapp, J. Lloyd-Evans, M. Marchesini and A. A. Watson, Astropart. Phys. 19 (2003) 47.
[24] H. Y. Dai, K. Kasahara, Y. Matsubara, M. Nagano and M. Teshima, J. Phys. G, 14 (1988) 793.
[25] E. E. Korosteleva, L. A. Kuzmichev and V. V. Prosin for the EAS-TOP Collaboration, in Proc. 29th Int. Cosmic Ray Conf., Pune, 6 (2005) 253.
[26] C. L. Pryke, Astropart. Phys. 14 (2001) 319.
[27] P. Sokolsky, J. Belz and the HiRes Collabboration, in Proc. 29th Int. Cosmic Ray Conf., Pune, 6 (2005) 381.
[28] M. Ave, L. Cazón, J. A. Hinton, J. Knapp, J. Lloyd-Evans and A. A. Watson, Astropart. Phys. 19 (2003) 61.
[29] Y. A. Gallant et al., in Proc. Eur. Cosmic Ray Symp. Lisbon 2006, CD-ROM (two papers).
[30] A. Haungs et al., Czech. J. Phys. 55 (2005).
[31] S. Ostapchenko, Phys.Lett. B 636 (2006) 40.
[32] S. Ostapchenko, Phys. Rev. D 74 (2006) 014026.
[33] T. Pierog and K. Werner, astro-ph 0611311.
[34] A. Furuhata et al., in Proc. 29th Int. Cosmic Ray Conf., Pune, 6 (2005) 329.
[35] L. A. Kuzmichev et al., in Proc. 29th Int. Cosmic Ray Conf., Pune, 8 (2005) 255.
[36] Y. Katayose et al., in Proc. 29th Int. Cosmic Ray Conf., Pune, 8 (2005) 157.
[37] M. Brüggemann et al., in Proc. Eur. Cosmic Ray Symp. Lisbon 2006, CD-ROM.